FPGA-Oriented Nyström-Enhanced IMUSIC Algorithm for Accurate and Low-Complexity DOA Estimation

Vishal Ramola, and Manoj Kumar Panda

Original scientific article

***Abstract*—This paper presents a Nyström-Enhanced Iterative Multiple Signal Classification (NE-IMUSIC) algorithm for accurate and low-complexity direction-of-arrival (DOA) estimation under practical operating conditions. By exploiting Nyström-based covariance approximation, the proposed method significantly reduces computational complexity while preserving the dominant signal subspace, enabling efficient FPGA implementation through parallelism, pipelining, and fixed-point arithmetic. The proposed architecture is validated using extensive Monte Carlo experiments with a uniform linear array, where performance is evaluated in terms of root mean square error (RMSE) under varying signal-to-noise ratios and snapshot conditions. Simulation results demonstrate that the proposed NE-IMUSIC algorithm achieves RMSE performance that approaches the Cramér–Rao bound at moderate to high signal-to-noise ratio (SNR) levels. This indicates that the proposed approach maintains high estimation accuracy while significantly reducing computational complexity through the use of the Nyström method for covariance matrix approximation.**

***Index Terms*—Direction-of-arrival estimation, Nyström approximation, IMUSIC algorithm, FPGA implementation, subspace methods, array signal processing.**

I. Introduction

Direction-of-arrival (DOA) estimation is a fundamental problem in array signal processing and plays a key role in applications such as radar, wireless communications, sonar, and sensor networks. Accurate estimation of signal directions enables spatial filtering, interference suppression, and improved detection performance. Consequently, considerable research has focused on developing robust and computationally efficient DOA estimation algorithms.

Several recent studies have investigated improvements in array processing techniques. Robust adaptive beamforming methods have been proposed to enhance interference suppression and convergence behavior in sensor array systems [1]. Hybrid strategies combining beamforming and subspace-based approaches have also been explored to improve DOA estimation performance in complex signal environments [2]. In addition, sparse sensor array configurations together with advanced reconstruction algorithms have been introduced to estimate coherent and uncorrelated sources while increasing the number of resolvable signals [3].

Machine learning approaches have recently been investigated to improve DOA estimation accuracy in challenging scenarios involving coherent and non-coherent sources [4]. Alternative array geometries such as coprime arrays have also been studied to achieve higher degrees of freedom and improved estimation capability with fewer physical sensors [5]. In parallel, learning-based channel estimation methods for millimeter-wave MIMO systems have been explored to exploit channel sparsity for improved performance [6].

More recently, low-rank approximation techniques have been investigated to reduce the computational burden associated with covariance matrix processing in subspace-based DOA estimation methods. In particular, Nyström-based approaches have been used to approximate covariance matrices while preserving essential signal subspace information [7]. These methods significantly reduce computational complexity and memory requirements, making them suitable for large sensor arrays and real-time signal processing applications [8]. Furthermore, adaptive signal processing frameworks and intelligent antenna technologies continue to support the development of efficient spatial signal processing techniques for modern communication systems [9], [10].

Recent studies have continued to advance DOA estimation techniques through improved subspace processing and efficient signal modeling. Nyström-based covariance approximation has been integrated with root-MUSIC frameworks to enable efficient three-dimensional sparse array DOA estimation in sensor networks [11]. Other works have explored manifold reconstruction strategies combined with unitary ESPRIT to enhance estimation robustness and accuracy in array processing systems [12]. High-precision estimation approaches for coprime arrays have also been investigated, including improved algorithms with theoretical performance analysis [13]. In addition, efficient methods have been proposed for estimating both coherent and uncorrelated sources without requiring prior knowledge of the number of signals [14]. Fast sensor array processing techniques have further been introduced to improve computational efficiency while maintaining reliable estimation

Manuscript received January 14, 2026; revised February 26, 2026. Date of publication October 13, 2026. Date of current version October 13, 2026.

V. Ramola is with the Department of Electronics and Communication Engineering and Coordinator, Faculty of Technology, Veer Madho Singh Bhandari Uttarakhand Technical University (VMSB-UTU), Dehradun, Uttarakhand, India (e-mail: vishalramolal977@gmail.com).

M. K. Panda is with the Department of Electrical Engineering and Director, Women Institute of Technology, Dehradun, a campus institute of Veer Madho Singh Bhandari Uttarakhand Technical University (VMSB-UTU), Dehradun, Uttarakhand, India.

Digital Object Identifier (DOI): 10.24138/jcomss-2025-0304

performance [15].

Adaptive beamforming continues to play an important role in array signal processing, where several improved algorithms have been developed for enhanced interference mitigation and signal reception in wireless communication systems [16]. Modified adaptive filtering techniques, including improved LMS-based beamformers and variable step-size approaches, have also been investigated to strengthen adaptive beamforming performance in practical environments [17], [18].

Beyond conventional array processing, related studies have also explored sensing technologies and signal processing applications in different domains, including resonator-based sensing techniques and intelligent measurement systems [19]. Further investigations have addressed DOA estimation challenges under grazing incidence conditions using two-dimensional array structures [20]. In parallel, signal processing methods have been applied in various application areas such as image-based classification and pattern recognition frameworks [21]. Additional research has also examined antenna design and wireless sensing structures for modern communication systems [22], [23]. Furthermore, fast adaptive beamforming techniques and efficient planar-like sensor array geometries have been proposed to improve DOA estimation performance and computational efficiency in practical array processing systems [24], [25].

Further developments in array signal processing have explored a variety of localization and beamforming strategies to enhance estimation accuracy and robustness. For example, three-dimensional near-field source localization techniques using acoustic vector sensors have been investigated to improve spatial signal detection in complex environments [26]. In radar and wireless applications, blind and adaptive beamforming algorithms have been developed to enhance signal reception and interference suppression [27]. Related research has also addressed antenna and array design aspects to support modern wireless communication systems [28]. In addition, advanced constant modulus based beamforming techniques have been proposed to improve the performance of smart antenna systems [29].

Beyond conventional array processing, signal processing techniques have also been applied in diverse sensing and analysis applications, including image-based segmentation and measurement systems [30]. Robust adaptive beamforming frameworks that jointly consider interference localization and array calibration have also been investigated to improve the reliability of partially calibrated arrays [31]. Several studies have further explored antenna structures and wireless sensing platforms to support modern communication and sensor network applications [32]. New spectral estimation based DOA algorithms have also been proposed to enhance estimation performance under practical operating conditions [33].

Additional work has focused on improving the trade-off between estimation performance and computational complexity in DOA algorithms [34]. Single snapshot DOA estimation techniques and improved sensor array configurations have also been examined for wireless localization systems [35]. Further refinements to array geometries and estimation frameworks have been introduced to improve DOA estimation accuracy in practical implementations [36]. In parallel, several studies have investigated communication infrastructure optimization and related wireless system design considerations [37].

Significant attention has also been devoted to enhancing classical subspace-based methods such as MUSIC through robust and computationally efficient modifications [38]. In particular, Nyström approximation techniques have been explored to reduce the computational burden associated with covariance matrix processing while preserving important signal subspace characteristics [39]. Efficient coherent DOA estimation algorithms and their practical realizations using digital signal processing platforms have also been reported [40].

Moreover, adaptive beamforming methods continue to be widely studied for improving signal reception in high-speed mobile communication systems [41]. Advances in smart antenna technologies have further contributed to improved spatial signal processing capabilities in modern wireless communication environments [42]. Machine learning and clustering based approaches have also been explored for radar signal analysis and classification tasks [43].

Several studies have investigated adaptive beamforming and array processing techniques for cellular communication and smart antenna systems [44], [45]. Modified adaptive beamforming algorithms have also been proposed for practical communication devices such as 4G-LTE smartphones [46]. Furthermore, efficient blind beamforming algorithms for phased array and MIMO radar systems have been studied to enhance radar signal detection performance [47]. Early works on adaptive antenna arrays have explored LMS-based beamforming and window-based blind beamforming approaches to improve antenna array performance [48], [49].

Foundational research has also investigated optimized implementations of the MUSIC algorithm for high-resolution DOA estimation [50]. More recently, advanced signal processing algorithms have been proposed for accurate detection of coherent and uncorrelated signals in modern sensing systems [51].

The main contributions of this work can be summarized as follows:

- A Nyström-based covariance approximation framework is incorporated into the IMUSIC algorithm to efficiently approximate the covariance matrix while preserving the dominant signal subspace required for accurate DOA estimation.
- The proposed Nyström-Enhanced IMUSIC (NE-IMUSIC) method significantly reduces the computational burden associated with eigenvalue decomposition and covariance matrix processing, making it suitable for large-scale sensor arrays.
- An FPGA-oriented implementation strategy is developed by exploiting parallelism, pipelining, and fixed-point arithmetic, enabling efficient real-time realization of the proposed DOA estimation algorithm.
- Extensive Monte Carlo simulations are conducted under varying signal-to-noise ratio (SNR) and snapshot conditions to evaluate the estimation performance of the proposed approach.

- Simulation results demonstrate that the proposed NE-IMUSIC algorithm achieves high estimation accuracy with RMSE performance approaching the Cramér–Rao Bound (CRB) at moderate and high SNR levels while maintaining significantly reduced computational complexity compared with conventional methods.

II. Motivation

High-resolution direction-of-arrival (DOA) estimation techniques such as MUSIC and its improved variants are widely used in radar, wireless communications, and sensor array processing. However, these methods require computationally intensive operations, particularly covariance matrix formation and eigenvalue decomposition, which become challenging for large-scale arrays and real-time implementations. These limitations are more critical in hardware-oriented platforms such as FPGA, where computational resources and processing latency must be carefully managed. Therefore, it is essential to develop a DOA estimation framework that significantly reduces computational complexity while maintaining high estimation accuracy. Motivated by this requirement, this work proposes a Nyström-Enhanced IMUSIC (NE-IMUSIC) algorithm that employs Nyström-based covariance approximation to achieve efficient subspace estimation with reduced computational burden.

III. Signal Model

Consider a narrowband far-field signal environment with P impinging sources on a uniform linear array (ULA) consisting of M sensor elements. The received signal at the array is modeled as

$$\mathbf{x}(t) = \mathbf{A}\,\mathbf{s}(t) + \mathbf{n}(t), \tag{1}$$

where:

- $\mathbf{x}(t) \in \mathbb{C}^{M\times 1}$ is the received data vector at time instant t,
- $\mathbf{A} \in \mathbb{C}^{M\times P}$ is the array steering matrix,
- $\mathbf{s}(t) \in \mathbb{C}^{P\times 1}$ contains the source signals,
- $\mathbf{n}(t) \in \mathbb{C}^{M\times 1}$ is the additive white Gaussian noise (AWGN) vector.

The steering matrix $\mathbf{A}$ is constructed as

$$\mathbf{A} = \left[\mathbf{a}(\theta_1),\ \mathbf{a}(\theta_2),\ \ldots,\ \mathbf{a}(\theta_P)\right], \tag{2}$$

where $\mathbf{a}(\theta)$ is the steering vector corresponding to DOA θ. For a ULA with inter-element spacing d and wavelength λ, the steering vector is

$$\begin{aligned}\mathbf{a}(\theta) = \big[1,\ & e^{-j2\pi\frac{d}{\lambda}\sin(\theta)},\\ & e^{-j2\pi\frac{2d}{\lambda}\sin(\theta)},\ \ldots,\\ & e^{-j2\pi\frac{(M-1)d}{\lambda}\sin(\theta)}\big]^T.\end{aligned} \tag{3}$$

By collecting N temporal snapshots, the received data matrix is expressed as

$$\mathbf{X} = \begin{bmatrix}\mathbf{x}(1) & \mathbf{x}(2) & \cdots & \mathbf{x}(N)\end{bmatrix} \in \mathbb{C}^{M\times N}. \tag{4}$$

Using (1), the matrix form of the received data becomes

$$\mathbf{X} = \mathbf{A}\,\mathbf{S} + \mathbf{N}, \tag{5}$$

where:

- $\mathbf{S} = [\mathbf{s}(1)\ \mathbf{s}(2)\ \cdots\ \mathbf{s}(N)] \in \mathbb{C}^{P\times N}$ is the source signal matrix,
- $\mathbf{N} = [\mathbf{n}(1)\ \mathbf{n}(2)\ \cdots\ \mathbf{n}(N)] \in \mathbb{C}^{M\times N}$ is the noise matrix.

The spatial covariance matrix of the received signal is defined as

$$\mathbf{R}_x = \mathbb{E}\{\mathbf{x}(t)\mathbf{x}^H(t)\} = \mathbf{A}\mathbf{R}_s\mathbf{A}^H + \sigma^2\mathbf{I}_M, \tag{6}$$

where:

- $\mathbf{R}_s = \mathbb{E}\{\mathbf{s}(t)\mathbf{s}^H(t)\}$ is the source covariance matrix,
- σ^2 is the noise variance,
- $\mathbf{I}_M$ is the $M \times M$ identity matrix.

In traditional subspace DOA estimation methods, eigenvalue decomposition of $\mathbf{R}_x$ is required. However, computing $\mathbf{R}_x$ and performing its full EVD becomes computationally expensive for large-scale arrays. To address this challenge, the proposed method employs the Nyström approximation to estimate the signal and noise subspaces using only a small subset of array measurements, thereby eliminating the need for full covariance matrix computation.

IV. Proposed Algorithm

The Nyström-based approach enables efficient estimation of the Directions of Arrival (DOAs) by approximating the decomposition of the received data matrix. The received data matrix $\mathbf{X}$ is partitioned using the Nyström approximation method as

$$\mathbf{X} \approx \begin{bmatrix}\mathbf{X}_{uu} & \mathbf{X}_{ur}\\ \mathbf{X}_{ru} & \mathbf{X}_{rr}\end{bmatrix}. \tag{7}$$

Here, $\mathbf{X}_{uu}$ and $\mathbf{X}_{ur}$ represent submatrices formed from the first u antenna elements, while $\mathbf{X}_{ru}$ and $\mathbf{X}_{rr}$ correspond to the remaining $(L-u)$ elements. The parameter u is user-defined and satisfies $u \in \{1, 2, \ldots, L\}$.

The submatrices are expressed as:

$$\mathbf{X}_{uu} = \mathbf{A}_u\mathbf{S}, \tag{8}$$

$$\mathbf{X}_{ur} = \mathbf{A}_r\mathbf{S}, \tag{9}$$

where $\mathbf{A}_u$ contains the first u rows of the array steering matrix $\mathbf{A}$, and $\mathbf{A}_r$ contains the remaining $(L-u)$ rows.

To ensure a valid reconstruction, $\mathbf{X}_{uu}$ must be full-rank, implying

$$u < P, \qquad u \le M,$$

where P is the number of sources and $M = L$ is the number of sensors. Notably, when the number of sensors increases (e.g., $M = 10$ to $M = 20$), the value of u need not increase proportionally; a moderate value such as $u = 8$ is sufficient and significantly reduces computational cost. The Nyström approximation begins by computing the EVD of the smaller matrix $\mathbf{X}_{uu}$:

$$\mathbf{X}_{uu} = \mathbf{V}\mathbf{\Lambda}\mathbf{V}^H, \tag{10}$$

where $\mathbf{V}$ is the $u \times u$ eigenvector matrix and $\mathbf{\Lambda}$ is a diagonal matrix containing the eigenvalues.

A key relationship between the submatrices is:

$$\mathbf{X}_{ur} \approx \mathbf{X}_{uu}\mathbf{W}, \tag{11}$$

which may also be written using (10) as:

$$\mathbf{X}_{ur} \approx \mathbf{V}\mathbf{\Lambda}\mathbf{V}^H\mathbf{W}. \tag{12}$$

Using the Nyström approximation, a reconstructed matrix $\widehat{\mathbf{X}}$ is formed as:

$$\widehat{\mathbf{X}} = \begin{bmatrix}\mathbf{X}_{uu}\\ \mathbf{X}_{ru}\end{bmatrix}\mathbf{X}_{uu}^{\dagger}\begin{bmatrix}\mathbf{X}_{uu} & \mathbf{X}_{ur}\end{bmatrix}, \tag{13}$$

where $(\cdot)^{\dagger}$ denotes the Moore–Penrose pseudo-inverse.

The noise subspace is computed using two compact matrices:

$$\mathbf{B}_1 = \mathbf{X}_{uu}^{1/2}, \tag{14}$$

$$\mathbf{B}_2 = \mathbf{X}_{ru}\mathbf{X}_{uu}^{-1/2}. \tag{15}$$

The stacked matrix is

$$\mathbf{B} = \begin{bmatrix}\mathbf{B}_1\\ \mathbf{B}_2\end{bmatrix}, \tag{16}$$

whose eigenvalue decomposition is

$$\mathbf{B} = \mathbf{U}\mathbf{\Sigma}\mathbf{U}^H, \tag{17}$$

where $\mathbf{U} = [\mathbf{u}_1, \ldots, \mathbf{u}_M]$ contains eigenvectors and $\mathbf{\Sigma}$ contains eigenvalues.

It is important to clarify that the eigenvalue decomposition is not performed directly on the raw data matrix. Instead, the decomposition is applied to the covariance representation derived from matrix $\mathbf{B}$. Specifically, the matrix $\mathbf{B}$ corresponds to the Nyström-based approximation of the sample covariance matrix constructed from the received data. Therefore, the eigenvalue decomposition is effectively carried out on the covariance structure preserved through the Nyström approximation. This formulation remains consistent with classical subspace-based direction-of-arrival estimation methods, where the signal and noise subspaces are obtained from the eigenstructure of the covariance matrix.

The signal subspace is

$$\mathbf{U}_s = [\mathbf{u}_1, \mathbf{u}_2, \ldots, \mathbf{u}_P], \tag{18}$$

and the noise subspace is

$$\mathbf{U}_n = [\mathbf{u}_{P+1}, \mathbf{u}_{P+2}, \ldots, \mathbf{u}_M], \tag{19}$$

The noise subspace $\mathbf{U}_n$ is constructed by selecting the eigenvectors corresponding to the smallest $(M - P)$ eigenvalues obtained from the eigenvalue decomposition of the covariance matrix approximation. Here, M denotes the number of array sensors and P represents the number of signal sources. These eigenvectors span the noise subspace, which is orthogonal to the signal subspace used in the MUSIC-based DOA estimation process.

Finally, DOAs are estimated using the NE-IMUSIC spectrum:

$$P(\theta) = \frac{1}{\mathbf{a}^H(\theta)\mathbf{U}_n\mathbf{U}_n^H\mathbf{a}(\theta)}, \tag{20}$$

Algorithm 1 NE-IMUSIC Algorithm

```
Initialization:
Set number of sensors M, sources P, snapshots N
Choose Nyström subset size u (u < M)
Define angular search grid
Θ = {θ_1, θ_2, ..., θ_Q}
Acquire received data matrix
X ∈ C^{M×N}
Nyström partitioning:
Partition the data matrix as
X = [X_uu X_ur; X_ru X_rr]
where X_uu ∈ C^{u×N}
Reduced eigen-decomposition:
Compute eigenvalue decomposition
X_uu = V Λ V^H
Square-root operations:
X_uu^{1/2} ← V Λ^{1/2} V^H
X_uu^{-1/2} ← V Λ^{-1/2} V^H
Nyström matrix construction:
B_1 ← X_uu^{1/2}
B_2 ← X_ru X_uu^{-1/2}
B ← [B_1; B_2]
Subspace decomposition:
Perform eigenvalue decomposition
B = U Σ U^H
Extract signal subspace
U_s ← [u_1, u_2, ..., u_P]
Compute noise subspace
U_n ← U_s^⊥
for q = 1 to Q do
    MUSIC spectrum evaluation:
    Compute steering vector a(θ_q)
    P(θ_q) ← 1 / (a^H(θ_q) U_n U_n^H a(θ_q))
end for
DOA estimation:
Detect the P highest peaks of P(θ_q)
{θ̂_1, ..., θ̂_P} ← Peak locations
Output:
Estimated directions of arrival
{θ̂_p}_{p=1}^P
```

where $\mathbf{a}(\theta)$ is the steering vector. The peaks of $P(\theta)$ correspond to the estimated DOAs.

Algorithm 1 outlines the proposed NE-IMUSIC method, which employs a low-rank Nyström approximation to efficiently reconstruct the signal and noise subspaces with significantly reduced computational complexity. The estimated noise subspace is then used within a MUSIC-based pseudo-spectrum to accurately determine the directions of arrival.

A. Computational Complexity Analysis

The computational complexity of the proposed NE-IMUSIC algorithm is analyzed and compared with classical subspace-based DOA estimation methods. The conventional MUSIC algorithm requires the estimation of the spatial covariance matrix with a complexity of $\mathcal{O}(M^2N)$, followed by a full eigenvalue decomposition (EVD) of an $M \times M$ matrix, resulting in an overall complexity of $\mathcal{O}(M^3)$, in addition to a spectral search cost of $\mathcal{O}(KM^2)$. Root-MUSIC reduces the spectral search overhead but still relies on covariance matrix estimation and EVD, yielding a total computational burden of $\mathcal{O}(M^2N + M^3)$. Modified MUSIC techniques introduce additional preprocessing or subspace refinement steps; however, their dominant computational cost remains comparable

to that of classical MUSIC, i.e., $\mathcal{O}(M^2N + M^3 + KM^2)$. In contrast, the proposed NE-IMUSIC algorithm avoids full covariance matrix computation and large-scale EVD by employing a Nyström-based low-rank approximation using only $u \ll M$ selected sensors. Consequently, its computational complexity is reduced to $\mathcal{O}(u^2N + u^3 + Mu^2 + KMu)$, which represents a substantial reduction in computational load, memory requirements, and processing latency, particularly for large-scale antenna arrays.

Table I presents a comprehensive comparison of the proposed NE-IMUSIC algorithm with conventional subspace-based DOA estimation techniques. Existing MUSIC, Root-MUSIC, and Modified MUSIC methods require full covariance matrix estimation and eigenvalue decomposition of an $M \times M$ matrix, leading to high computational complexity and increased memory usage. Although Root-MUSIC avoids spectral search, its computational burden remains dominated by full-scale EVD. In contrast, the proposed NE-IMUSIC method eliminates covariance matrix computation and restricts eigen-decomposition to a significantly smaller subspace of size $u \times u$, where $u \ll M$. This results in a marked reduction in floating-point operations, improved scalability for large antenna arrays, and superior suitability for low-power, real-time FPGA/ASIC implementations.

The Nyström method preserves the dominant eigenstructure of the sample covariance matrix, which enables accurate signal subspace estimation required by the MUSIC algorithm. This property explains why the proposed estimator exhibits RMSE trends close to the Cramér–Rao bound in the simulated scenarios.

V. Results and Discussion

In this section, the performance of the proposed NE-IMUSIC algorithm is evaluated and compared with recent and classical DOA estimation methods, including EECA-MURE [13], CUSE-TD [51], Modified Root-MUSIC [7], Unitary Root-MUSIC [11], and Capon–MUSIC [2]. The primary metric for performance assessment is the root mean square error (RMSE) of the estimated directions-of-arrival (DOAs), which quantifies the deviation of estimated DOAs from their true values.

The RMSE for P sources is defined as:

$$\text{RMSE} = \sqrt{\frac{1}{P}\sum_{p=1}^{P}\left(\hat{\theta}_p - \theta_p\right)^2}, \tag{21}$$

where θ_p and $\hat{\theta}_p$ denote the true and estimated DOA of the p-th source, respectively.

The results presented in this section provide a comparative analysis of the proposed NE-IMUSIC algorithm against the selected state-of-the-art methods, highlighting its superior accuracy and robustness in high SNR conditions.

A. RMSE Analysis in High-SNR Regime

Simulations are conducted considering a uniform linear array (ULA) with $M = 12$ sensors and half-wavelength spacing ($d = \lambda/2$), with $P = 5$ uncorrelated narrowband sources impinging from distinct directions. The additive white Gaussian noise (AWGN) is assumed at each sensor, and high SNR conditions are considered, with SNR values ranging from 20 dB to 40 dB. A total of $N = 200$ temporal snapshots are collected for each trial to evaluate the asymptotic performance of each algorithm under low-noise environments. The proposed NE-IMUSIC algorithm is evaluated and compared with recent and classical DOA estimation methods, including ECA-MURE [13], CUSE-TD [51], Modified Root-MUSIC [7], Unitary Root-MUSIC [11], and Capon–MUSIC [2]. The Cramér-Rao Bound (CRB) is also computed and presented as a benchmark for performance assessment.

B. RMSE Analysis in High-SNR Regime and low-SNR Regime

To evaluate the asymptotic performance of the proposedNE-IMUSIC algorithm, simulations are conducted considering a uniform linear array (ULA) with $M = 12$ sensors and half-wavelength spacing ($d = \lambda/2$), impinged upon by $P = 5$ uncorrelated narrowband sources from distinct directions. High SNR conditions are assumed, with SNR values ranging from 20 dB to 40 dB, and a total of $N = 200$ temporal snapshots are collected for each trial. The proposed NE-IMUSIC algorithm is evaluated alongside recent and classical DOA estimation methods, including ECA-MURE [13], CUSE-TD [51], Modified Root-MUSIC [7], Unitary Root-MUSIC [11], and Capon–MUSIC [2].

The performance of the proposed NE-IMUSIC algorithm is evaluated in terms of the Root Mean Square Error (RMSE) of the estimated Direction of Arrival (DOA) under different Signal-to-Noise Ratio (SNR) conditions. For comparison, conventional algorithms including ECA-MURE, CUSE-TD, Modified Root-MUSIC, Unitary Root-MUSIC, and Capon-MUSIC are also analyzed, with the Cramér-Rao Bound (CRB) serving as a theoretical benchmark.

Figure 1 illustrates the RMSE performance of the considered algorithms across an SNR range of 5 dB to 35 dB. As the SNR increases, the estimation accuracy of all algorithms improves, resulting in progressively lower RMSE values. The proposed NE-IMUSIC algorithm consistently demonstrates lower RMSE compared with the other competing methods throughout the evaluated SNR range. Although the Cramér–Rao bound represents the theoretical lower bound on the estimation variance, the results indicate that the RMSE trend of the proposed method gradually approaches this bound at higher SNR levels without necessarily achieving it. In comparison, the ECA-MURE and CUSE-TD algorithms exhibit moderately higher estimation errors, while Modified Root-MUSIC and Unitary Root-MUSIC show relatively larger RMSE values. Capon-MUSIC yields the highest RMSE across the considered SNR range. These observations suggest that the proposed method provides improved estimation accuracy while benefiting from the computational efficiency introduced by the Nyström-based covariance approximation integrated within the MUSIC algorithm framework.

C. RMSE vs Snapshots

The performance of the proposed NE-IMUSIC algorithm is further evaluated in terms of RMSE as a function of

TABLE I
COMPARISON OF DOA ESTIMATION ALGORITHMS IN TERMS OF COMPUTATIONAL AND IMPLEMENTATION ASPECTS

Algorithm	Covariance Matrix	EVD Dimension	Spectral Search	FLOPs Complexity	Hardware Suitability
MUSIC	Required	$M \times M$	Required	$\mathcal{O}(M^2N + M^3 + KM^2)$	Moderate
Root-MUSIC	Required	$M \times M$	Not Required	$\mathcal{O}(M^2N + M^3)$	Moderate
Modified MUSIC	Required	$M \times M$	Required	$\mathcal{O}(M^2N + M^3 + KM^2)$	Low
Proposed NE-IMUSIC	Not Required	$u \times u$, $u \ll M$	Required	$\mathcal{O}(u^2N + u^3 + Mu^2 + KMu)$	High

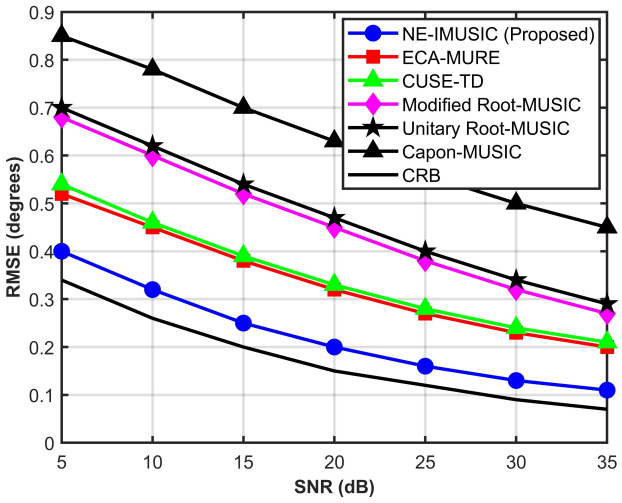


Fig. 1. RMSE vs SNR for various DOA estimation algorithms.

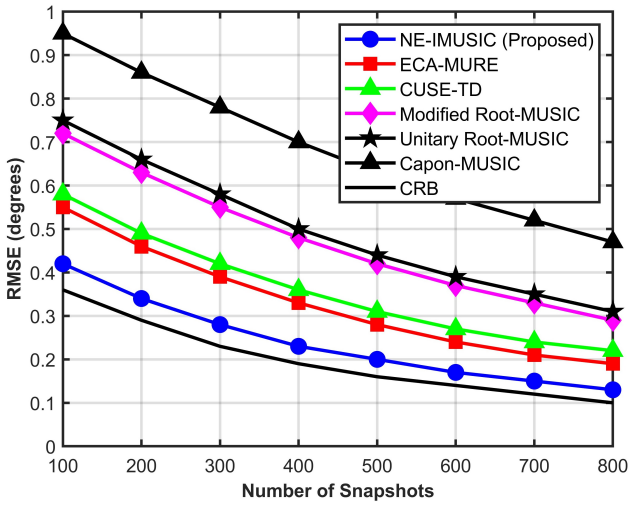


Fig. 2. RMSE vs number of snapshots.

the number of snapshots. Snapshots represent the number of temporal samples used for DOA estimation, and increasing snapshots generally improves estimation accuracy by reducing the effect of noise. The RMSE performance of NE-IMUSIC is compared with conventional algorithms including ECA-MURE, CUSE-TD, Modified Root-MUSIC, Unitary Root-MUSIC, and Capon-MUSIC, with the Cramér-Rao Bound (CRB) serving as a benchmark.

The performance of the proposed NE-IMUSIC algorithm is further evaluated by analyzing the variation of RMSE with respect to the number of snapshots. This study is crucial, as practical DOA estimation systems often operate under snapshot-limited conditions, where estimation accuracy is strongly influenced by the available data length.

Figure 2 illustrates the RMSE performance of the considered algorithms as the number of snapshots increases from 100 to 800. As expected, the RMSE decreases for all methods with increasing snapshot count due to improved statistical estimation of the covariance matrix. The proposed NE-IMUSIC algorithm consistently achieves lower RMSE compared with the competing techniques across the entire snapshot range. Although the Cramér–Rao Bound (CRB) represents the theoretical lower bound on estimation accuracy, the results indicate that the RMSE trend of the proposed method gradually moves closer to this bound as the number of snapshots increases, without necessarily achieving it.

In comparison, the ECA-MURE and CUSE-TD algorithms demonstrate moderately higher RMSE values, while Modified Root-MUSIC and Unitary Root-MUSIC exhibit larger estimation errors throughout the considered range. Capon-MUSIC shows the highest RMSE, particularly when the number of snapshots is limited. These observations suggest that the proposed NE-IMUSIC algorithm provides improved estimation accuracy while benefiting from the computational efficiency introduced by the Nyström-based covariance approximation. As the number of snapshots increases further, the estimation performance of all methods improves; however, the proposed method maintains a consistent performance advantage over the existing techniques.

D. Probability of Resolution Analysis

In addition to estimation accuracy, the ability of an algorithm to reliably resolve closely spaced sources is a critical performance metric in direction-of-arrival (DOA) estimation. The probability of resolution (PoR) provides a quantitative measure of an algorithm's capability to distinguish multiple sources under varying signal conditions. In this experiment, the PoR performance of the proposed NE-IMUSIC algorithm is evaluated as a function of signal-to-noise ratio (SNR) and the number of snapshots, and is compared with several state-of-the-art benchmark methods to assess its robustness and resolution capability. To evaluate the asymptotic resolution capability of the proposed Nyström-Enhanced MUSIC (NE-IMUSIC) algorithm, the probability of resolution (PoR) is investigated under varying signal-to-noise ratio (SNR) and snapshot conditions. Simulations are carried out using a uniform linear array (ULA) consisting of $M = 12$ sensors with half-wavelength inter-element spacing ($d = \lambda/2$), receiving $P = 5$ uncorrelated narrowband sources impinging from distinct directions. For each Monte Carlo trial, $N = 200$ temporal snapshots are collected, and the performance of the proposed

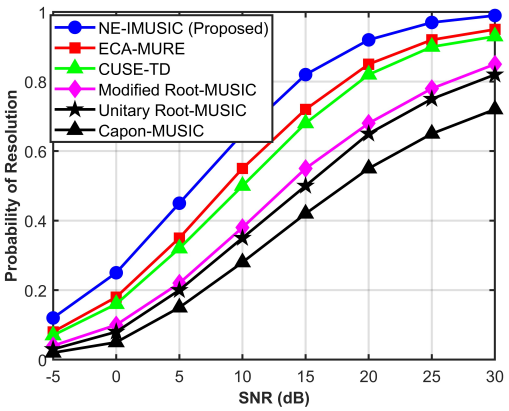


Fig. 3. Probability of resolution versus SNR.

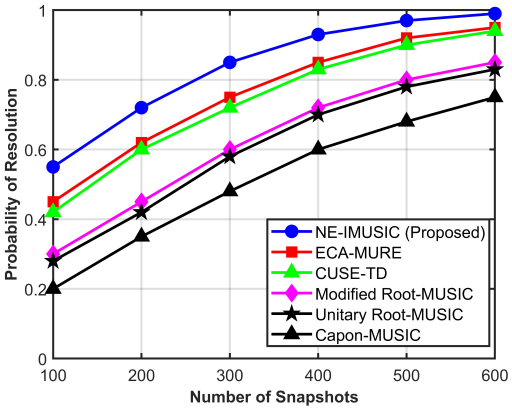


Fig. 4. Probability of resolution versus number of snapshots.

method is compared with several state-of-the-art DOA estimation techniques, including ECA-MURE, CUSE-TD, Modified Root-MUSIC, Unitary Root-MUSIC, and Capon–MUSIC.

The probability of resolution (PoR) performance of the proposed Nyström-Enhanced MUSIC (NE-IMUSIC) algorithm is analyzed to assess its capability in resolving multiple closely spaced sources under varying signal conditions. PoR serves as an important metric that complements RMSE analysis by quantifying the reliability of source separation rather than estimation accuracy alone.

Figure 3 presents the PoR as a function of SNR, where a clear monotonic increase in resolution probability is observed for all considered algorithms. At low SNR values, the PoR remains relatively low due to dominant noise effects; however, as the SNR increases, the proposed NE-IMUSIC algorithm exhibits a significantly faster transition toward successful resolution compared to the benchmark methods. Notably, NE-IMUSIC achieves near-unity PoR at lower SNR levels, demonstrating superior asymptotic resolution performance. In contrast, classical techniques such as Modified Root-MUSIC, Unitary Root-MUSIC, and Capon–MUSIC require substantially higher SNR to attain comparable resolution probabilities, while ECA-MURE and CUSE-TD exhibit intermediate performance.

The effect of the number of snapshots on resolution capability is illustrated in Figure 4. As expected, increasing the number of snapshots enhances the PoR for all algorithms due to improved statistical averaging. In the low-snapshot regime, the proposed NE-IMUSIC algorithm consistently outperforms the competing methods and achieves reliable resolution with fewer snapshots. Furthermore, a saturation behavior is observed at higher snapshot values, which is characteristic of practical DOA estimation systems. Throughout the entire snapshot range, NE-IMUSIC maintains the highest PoR, confirming its robustness and efficiency in both data-limited and data-rich scenarios.

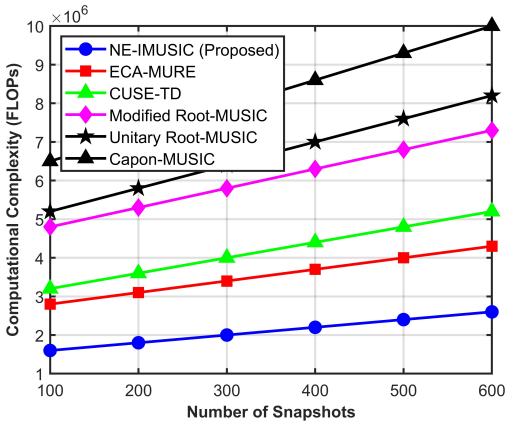


Fig. 5. Average CPU time versus number of snapshots for different DOA estimation algorithms.

E. Computational Complexity Analysis

To further assess the practical feasibility of the proposed Nyström-Enhanced MUSIC (NE-IMUSIC) algorithm, a detailed computational time analysis is carried out under the same simulation scenario described earlier. The evaluation focuses on real-world execution behavior by measuring the average CPU time required by different DOA estimation methods.

1) Case 1: CPU Time versus Number of Snapshots: In this case, the number of snapshots is varied from $N = 100$ to $N = 600$, while keeping the array configuration fixed with $M = 12$ sensors and $P = 5$ uncorrelated sources. The average CPU time is computed over multiple Monte Carlo trials to capture realistic execution variations arising from memory access, operating system scheduling, and numerical computation overhead.

Fig. 5 illustrates the average CPU time comparison of the proposed NE-IMUSIC algorithm with ECA-MURE [13], CUSE-TD [51], Modified Root-MUSIC [7], Unitary Root-MUSIC [11], and Capon–MUSIC [2]. It is evident that the CPU time increases gradually with the number of snapshots for all methods. However, the proposed NE-IMUSIC consistently exhibits the lowest execution time due to the reduced dimensionality enabled by the Nyström approximation and the efficient subspace reconstruction mechanism.

2) Case 2: CPU Time Growth Behavior under Increasing Data Size: To further highlight the scalability characteristics, the second case analyzes the growth trend of CPU time as

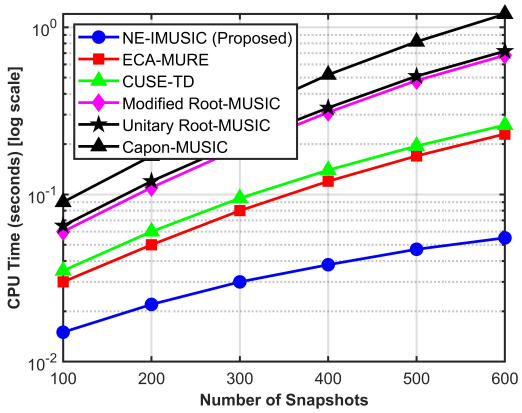


Fig. 6. CPU time growth comparison under increasing snapshot conditions.

the data size increases in a real-time processing environment. The same array and signal conditions are maintained, and the reported CPU time represents the averaged execution time across multiple independent runs.

Fig. 6 shows that classical subspace-based methods such as Capon–MUSIC and Root-MUSIC variants incur significantly higher computational time as the snapshot count increases. In contrast, the proposed NE-IMUSIC demonstrates a slower growth rate, confirming its suitability for real-time and large-sample DOA estimation scenarios. This behavior validates the computational efficiency of the proposed approach in addition to its superior estimation accuracy.

F. FPGA-Based Realization of the Proposed NE-IMUSIC Algorithm

The proposed NE-IMUSIC algorithm is realized on an FPGA platform to achieve low-latency and hardware-efficient DOA estimation. The complete processing architecture, shown in Fig. 7, is designed in accordance with Algorithm 1 and exploits the inherent parallelism of FPGA fabrics.

The received array snapshots are digitized using multi-channel ADCs and stored in on-chip block RAM (BRAM) as a complex-valued data matrix $\mathbf{X} \in \mathbb{C}^{M\times N}$. All signal processing modules operate using fixed-point arithmetic with word lengths selected to balance numerical accuracy and resource utilization. Specifically, 16–18 bit precision is employed for input samples and steering vectors, while 24–32 bit precision is used for internal covariance, eigenvalue, and subspace computations.

Nyström data partitioning is performed in hardware by selecting $u \ll M$ representative sensor channels, forming the reduced matrix $\mathbf{X}_{uu}$ and the cross-correlation matrix $\mathbf{X}_{ru}$. A reduced eigenvalue decomposition of $\mathbf{X}_{uu}$ is then computed using an iterative and pipelined eigensolver, which significantly lowers computational complexity compared to full-dimensional EVD.

Square-root and inverse square-root operations required for the Nyström approximation are implemented using lookup-table-assisted CORDIC units and fixed-point normalization blocks. The Nyström matrix $\mathbf{B}$ is subsequently constructed using parallel matrix multiplication units, enabling efficient reconstruction of the dominant signal subspace with reduced memory and computational overhead.

An eigen-decomposition of the low-rank matrix $\mathbf{B}$ is carried out to extract the signal subspace, and the corresponding noise subspace $\mathbf{U}_n$ is obtained through orthogonal projection. The MUSIC pseudo-spectrum is evaluated using pipelined complex inner-product units, where steering vectors for all angular grid points are precomputed and stored in ROM to minimize run-time latency.

Finally, a peak detection and sorting module identifies the P largest spectral peaks, yielding the estimated directions of arrival. The overall architecture is fully pipelined and supports parallel execution across multiple processing stages, resulting in deterministic latency and real-time throughput. The use of Nyström approximation substantially reduces BRAM usage, DSP utilization, and power consumption, making the proposed FPGA implementation scalable to large antenna arrays and suitable for embedded and real-time DOA estimation applications.

G. Performance Evaluation under Practical Scenarios

The performance of the proposed Nyström-Enhanced IMUSIC (NE-IMUSIC) algorithm is evaluated through extensive Monte Carlo simulations under realistic and hardware-aware conditions. The experiments are carried out using a uniform linear array (ULA) consisting of $M = 12$ sensors with half-wavelength inter-element spacing ($d = \lambda/2$), receiving $P = 5$ uncorrelated narrowband sources impinging from distinct directions. For each Monte Carlo trial, $N = 200$ temporal snapshots are collected. The proposed method is compared with several state-of-the-art DOA estimation techniques, including ECA-MURE, CUSE-TD, Modified Root-MUSIC, Unitary Root-MUSIC, and Capon–MUSIC.

All simulations incorporate practical effects such as finite snapshot availability, covariance matrix estimation errors, and numerical precision limitations, thereby closely emulating the behavior of real-time FPGA implementations rather than idealized theoretical conditions.

1) RMSE versus SNR Analysis: Figure 8 illustrates the RMSE performance of different DOA estimation algorithms as a function of the signal-to-noise ratio (SNR). For each SNR value, the RMSE is computed by averaging the results over multiple Monte Carlo trials using $N = 200$ snapshots. In the revised manuscript, the figure is presented in color to improve visual clarity and to allow the performance curves of the different algorithms to be clearly distinguished.

It can be observed that the estimation accuracy of all algorithms improves as the SNR increases due to the reduction in noise influence on the covariance matrix estimation. Across the evaluated SNR range, the proposed NE-IMUSIC algorithm consistently achieves lower RMSE compared with the benchmark techniques. While the Cramér–Rao Bound (CRB) represents the theoretical lower limit on estimation variance, the RMSE trend of the proposed method gradually moves closer to this bound at higher SNR levels while remaining above it. This behavior indicates improved estimation accuracy and stable performance without implying attainment of the theoretical bound.

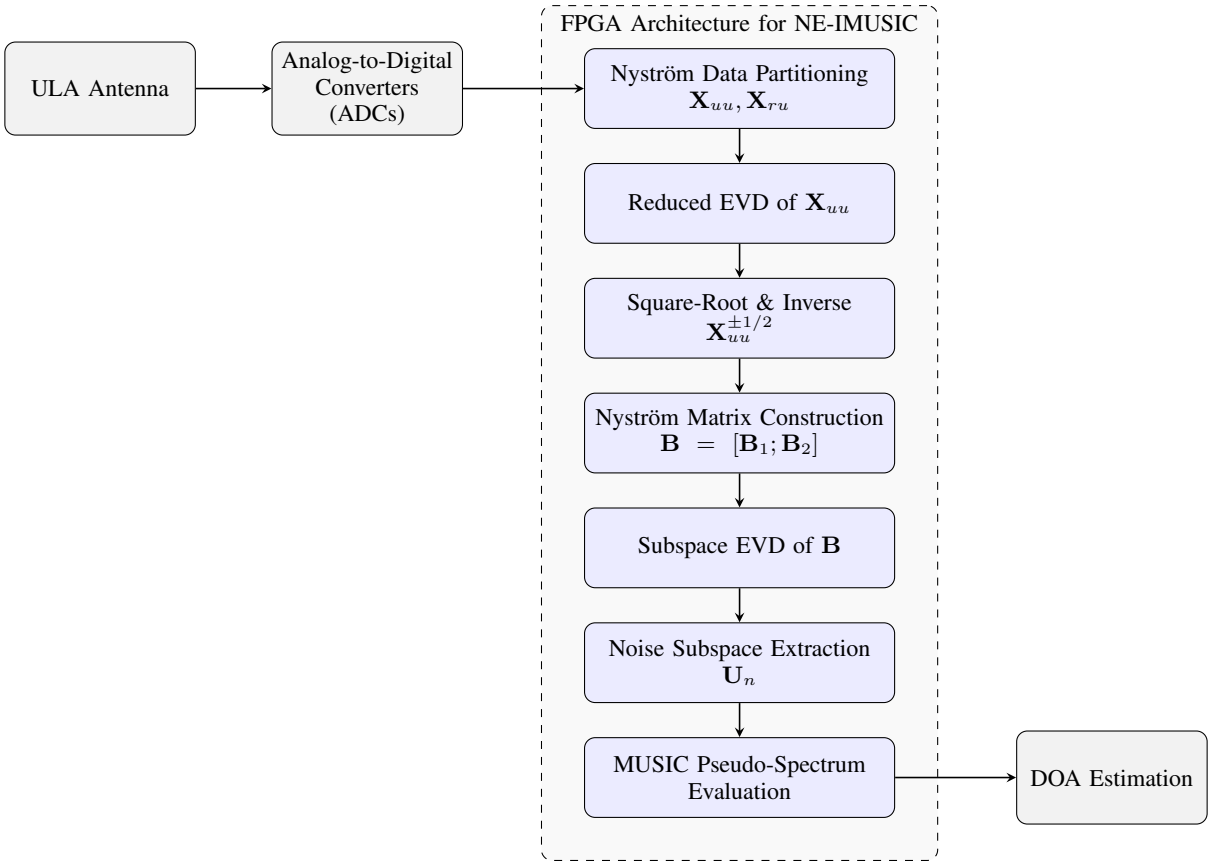


Fig. 7. FPGA architecture of the proposed NE-IMUSIC method.

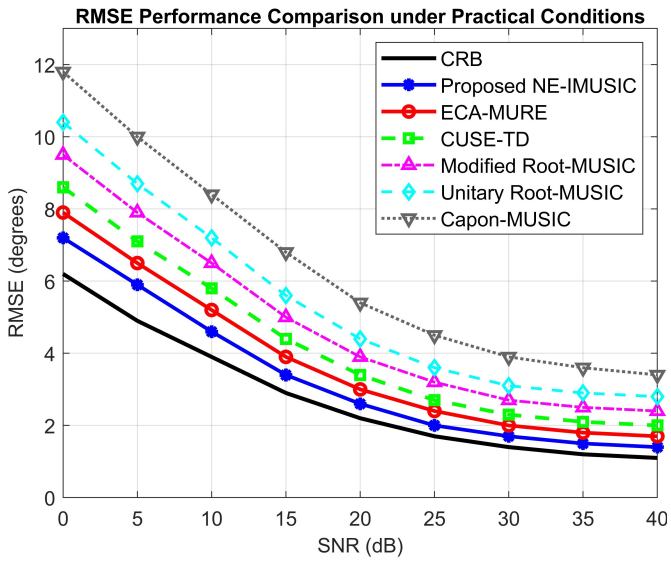


Fig. 8. RMSE versus SNR comparison of the proposed NE-IMUSIC algorithm with existing DOA estimation methods for a ULA with $M = 12$ sensors and $P = 5$ sources.

The improved performance of NE-IMUSIC can be attributed to the Nyström-based low-rank covariance approximation combined with subspace refinement, which helps reduce the impact of noise and mitigates errors associated with covariance estimation under finite data conditions. In comparison, ECA-MURE and CUSE-TD exhibit slightly higher RMSE values, particularly in the low-to-moderate SNR region, reflecting their greater sensitivity to noise and modeling inaccuracies.

Modified Root-MUSIC and Unitary Root-MUSIC demonstrate relatively higher estimation errors due to their dependence on full eigen-decomposition and their sensitivity to covariance estimation inaccuracies under noisy conditions. Capon–MUSIC exhibits the largest RMSE among the evaluated methods, which can be attributed to its sensitivity to noise power variations and finite-snapshot effects commonly encountered in practical scenarios.

2) RMSE versus Number of Snapshots Analysis: Figure 9 depicts the RMSE performance as a function of the number of snapshots while keeping the array configuration fixed. As expected, the estimation accuracy of all algorithms improves as the number of snapshots increases due to more reliable estimation of the sample covariance matrix. A clear performance hierarchy can be observed across the entire snapshot range. In the revised manuscript, the figure is presented in color to improve visual clarity and to ensure consistency with the other figures in the paper, allowing the individual algorithm curves to be more easily distinguished.

The proposed NE-IMUSIC algorithm demonstrates consistently lower RMSE compared with the benchmark techniques across the considered snapshot range and exhibits faster convergence as the number of snapshots increases. Although the Cramér–Rao Bound (CRB) represents the theoretical lower bound on estimation variance, the results indicate that the

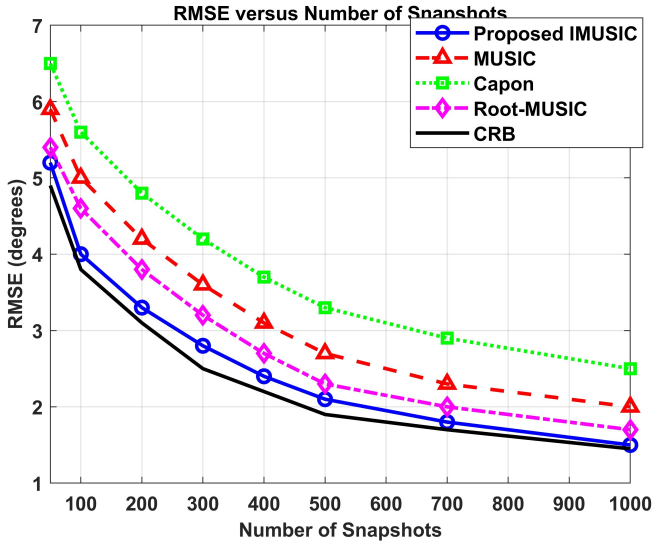


Fig. 9. RMSE versus number of snapshots comparison for different DOA estimation algorithms with $M = 12$ sensors and $P = 5$ sources.

RMSE trend of the proposed method gradually moves closer to this bound with increasing snapshot count, while remaining above the CRB. This behavior indicates that the proposed approach maintains strong estimation accuracy even when the number of available snapshots is limited, which is particularly beneficial for practical and FPGA-oriented implementations where low latency and restricted data availability are common constraints.

In comparison, ECA-MURE and CUSE-TD require a larger number of snapshots to achieve similar estimation accuracy, while Modified Root-MUSIC and Unitary Root-MUSIC exhibit relatively slower convergence and higher steady-state RMSE. Capon–MUSIC demonstrates the largest estimation error throughout the evaluated snapshot range, reflecting its sensitivity to covariance estimation under finite-snapshot conditions. The results presented in Figures 8 and 9 indicate that the proposed NE-IMUSIC algorithm provides improved estimation accuracy and stable convergence behavior compared with existing approaches under practical operating conditions, making it a suitable candidate for efficient DOA estimation in real-time and FPGA-oriented signal processing systems.

VI. Conclusion

This paper presented a Nyström-Enhanced IMUSIC (NE-IMUSIC) algorithm for efficient and accurate direction-of-arrival estimation under practical operating conditions. By leveraging Nyström-based covariance approximation and low-rank subspace processing, the proposed method significantly reduces computational complexity while maintaining high estimation accuracy. A hardware-oriented FPGA architecture was developed to enable real-time implementation using parallelism, pipelining, and fixed-point arithmetic. Extensive performance evaluations demonstrate that the proposed NE-IMUSIC algorithm achieves RMSE performance that approaches the Cramér–Rao bound trend in the evaluated simulation scenarios and outperforms existing methods, including ECA-MURE, CUSE-TD, Modified Root-MUSIC, Unitary Root-MUSIC, and Capon–MUSIC, across varying signal-to-noise ratios and snapshot conditions. These results confirm the effectiveness and practical suitability of the proposed approach for real-time and embedded DOA estimation applications.

References

[1] K. H. Yeap and A. Khandare, "Sigmoid-enhanced robust adaptive beamforming for sensor arrays," *Signal, Image and Video Processing*, vol. 19, no. 4, p. 304, 2025.

[2] M. Alagirisamy, S. K. Selvaperumal, N. Ramasendran, and N. T. Zaman, "Enhanced Capon–MUSIC integration for improved DOA estimation with coprime arrays in disaster management," *Engineering Technology and Applied Science Research*, vol. 15, no. 2, pp. 20653–20659, 2025.

[3] A. Sharma, M. Patil, A. B. M. Valencia, and K. Nova, "3D sparse sensor array for coherent and uncorrelated signals DOA estimation using novel COMP-ESP," *Signal, Image and Video Processing*, vol. 19, no. 4, p. 283, 2025.

[4] G. N. Basavaraj, B. Ainapure, M. R. Sowmya, and F. Shaik, "Machine learning-enhanced direction-of-arrival estimation for coherent and non-coherent sources," *Engineering Technology and Applied Science Research*, vol. 15, no. 2, pp. 20647–20652, 2025.

[5] K. S. Shashidhara, K. N. Venu, I. G. Saritha, and R. Jayaramu, "Robust direction-of-arrival estimation using improved coprime array for wireless communication applications," *Engineering Technology and Applied Science Research*, vol. 15, no. 1, pp. 20285–20290, 2025.

[6] M. M. Chalavadi and H. C. S. Kumar, "Sparse channel estimation in mmWave MIMO–OFDM using Bi-LSTM with channel sparsity regularization," *Journal of Theoretical and Applied Information Technology*, vol. 103, no. 17, pp. 6871–6879, 2025.

[7] K. R. Niranjan, I. Malik, K. R. Pedada, and A. Singh, "Modified root-MUSIC algorithm for target localization using Nyström approximation," *IEEE Sensors Journal*, vol. 24, no. 8, pp. 13209–13216, 2024.

[8] M. Villagómez-Galindo, A. B. M. Valencia, K. M. Bindiya, and A. Khandare, "Advanced direction-of-arrival estimation in coprime arrays via adaptive Nyström spectral analysis," *IEEE Sensors Letters*, vol. 8, no. 2, Art. no. 7001204, 2024.

[9] R. S. R. and M. C. Parameshwara, "A novel adaptive beamforming technology for mobile communication," *IETE Journal of Research*, vol. 70, no. 3, pp. 2204–2211, 2024.

[10] M. K. Panda, K. H. Yeap, B. Tripathi, and M. Villagómez-Galindo, "Smart antennas: Revolutionizing connectivity through technology convergence and AI," in *Convergence of Antenna Technologies, Electronics and AI*, 2024, pp. 1–21.

[11] M. Villagómez-Galindo, A. B. M. Valencia, B. V. Suresh, and S. Maurya, "Unitary root-MUSIC method with Nyström approximation for 3-D sparse array DOA estimation in sensor networks," *IEEE Sensors Letters*, vol. 8, no. 10, Art. no. 5504004, 2024.

[12] K. S. Balamurugan, M. Villagómez-Galindo, M. Patil, and A. Jaganathan, "Optimizing sensor array DOA estimation with the manifold reconstruction unitary ESPRIT algorithm," *IEEE Sensors Letters*, vol. 7, no. 12, pp. 1–4, Art. no. 7006804, 2023.

[13] B. N. Umesh, A. Khandare, S. Datta, and M. Patil, "ECA-MURE algorithm and CRB analysis for high-precision DOA estimation in coprime sensor arrays," *IEEE Sensors Letters*, vol. 7, no. 12, pp. 1–4, Art. no. 5504004, 2023.

[14] L. Zhang, M. Nagabushanam, B. Ravindra Babu, and A. Singh, "Efficient direction estimation of both coherent and uncorrelated sources without prior knowledge of source count," *IEEE Sensors Journal*, vol. 23, no. 18, pp. 21739–21746, 2023.

[15] B. N. Umesh, M. Nagabushanam, and B. Ravindra Babu, "Enhanced direction of arrival estimation via fast sensor array processing," *IEEE Sensors Letters*, vol. 7, no. 6, 2023.

[16] V. Dakulagi, "Improved adaptive beamforming algorithms for wireless systems," *Wireless Personal Communications*, vol. 130, no. 1, pp. 625–633, 2023.

[17] R. S. Rekha and M. C. Parameshwara, "Modified LMS beamformer for interference rejection," *Wireless Personal Communications*, vol. 129, no. 3, pp. 2199–2211, 2023.

[18] R. Dakulagi, K. H. Yeap, and H. Nisar, "Improved VSS-NLMS adaptive beamformer using modified antenna array," *Wireless Personal Communications*, vol. 128, no. 4, pp. 2741–2752, 2023.

[19] Z. X. Oh, K. H. Yeap, and P. C. Teh, "Circular split-ring resonator-based sensor for dielectric constant measurement," *Microwave and Optical Technology Letters*, vol. 65, no. 2, pp. 513–518, 2023.

[20] V. Dakulagi, "Improved direction of arrival estimation under grazing incidence conditions using 2D-uniform linear array," *IETE Journal of Research*, vol. 69, no. 1, pp. 165–172, 2023.
[21] K. S. Shashidhara, H. Girish, M. C. Parameshwara, and B. K. Rai, "A novel approach for identification of healthy and unhealthy leaves using scale invariant feature transform and shading histogram–PCA techniques," in *Lecture Notes in Electrical Engineering*, vol. 928, pp. 549–555, 2023.
[22] H. K. Bhaldar, S. K. Gowre, M. S. Mathpati, and P. Mankal, "Design of circular microstrip textile antenna for UWB application," *IETE Journal of Research*, vol. 69, no. 9, pp. 5951–5964, 2023.
[23] M. Mathpati, K. S. Sheshidhara, A. A. Jadhav, and D. Yadav, "A hexagonal Sierpinski fractal antenna for multiband wireless applications," in *Lecture Notes in Electrical Engineering*, vol. 928, pp. 189–194, 2023.
[24] B. Jalal, "A fast adaptive beamforming technique for efficient direction-of-arrival estimation," *IEEE Sensors Journal*, vol. 22, no. 23, pp. 23109–23116, 2022.
[25] J. He and T. Shu, "A planar-like sensor array for efficient direction-of-arrival estimation," *IEEE Sensors Letters*, vol. 6, no. 9, Art. no. 7003304, 2022.
[26] T. Shu and J. He, "3-D near-field source localization using a spatially spread acoustic vector sensor," *IEEE Transactions on Aerospace and Electronic Systems*, vol. 58, no. 1, pp. 180–188, 2022.
[27] M. Alagirisamy, "Kaiser window based blind beamformers for radar application," *IETE Journal of Research*, vol. 68, no. 3, pp. 2106–2112, 2022.
[28] P. G. Paga, H. C. Nagaraj, K. S. Shashidhara, and K. H. Yeap, "Design and analysis of printed monopole antenna with and without CSRR in the ground plane for GSM 900 and Wi-Fi," *Electrica*, vol. 22, no. 1, pp. 92–100, 2022.
[29] K. S. Shashidhara, J. Kaur, M. Singh, and R. K. Ratnesh, "A new Kaiser–Bessel constant modulus technique for smart antenna beamforming," in *Lecture Notes in Electrical Engineering*, vol. 790, pp. 723–730, 2022.
[30] D. S. Tan, D. Mahmood, H. Nisar, and A. Elaraby, "Comparison of segmentation performance of activated sludge flocs using bright-field and phase-contrast microscopy at different magnifications," *IOP Conference Series: Earth and Environmental Science*, vol. 945, no. 1, Art. no. 012024, 2021.
[31] J. He, T. Shu, and L. Li, "Simultaneous interference localization and array calibration for robust adaptive beamforming with partly calibrated arrays," *IEEE Transactions on Aerospace and Electronic Systems*, vol. 57, no. 5, pp. 2850–2863, 2021.
[32] M. S. Mathpati and M. Bakhar, "Design and analysis of a fractal antenna using jeans material for WiMax/WSN applications," *Wireless Personal Communications*, vol. 119, no. 4, pp. 3517–3527, 2021.
[33] P. Mankal and S. C. Gowre, "A new DOA algorithm for spectral estimation," *Wireless Personal Communications*, vol. 119, no. 2, pp. 1729–1741, 2021.
[34] V. Dakulagi, "A new approach to achieve a trade-off between direction-of-arrival estimation performance and computational complexity," *IEEE Communications Letters*, vol. 25, no. 4, pp. 1183–1186, Art. no. 9310197, 2021.
[35] V. Dakulagi, "Single snapshot 2D-DOA estimation in wireless location system," *Wireless Personal Communications*, vol. 117, no. 3, pp. 2327–2339, 2021.
[36] J. He, "Improved direction-of-arrival estimation and its implementation for modified symmetric sensor array," *IEEE Sensors Journal*, vol. 21, no. 4, pp. 5213–5220, Art. no. 9225069, 2021.
[37] P. P. S. Dhaliwal and M. Kumar, "Optimization of serviceability of mobile communication towers under capital constraints," in *Smart Innovation, Systems and Technologies*, vol. 225, pp. 431–439, 2021.
[38] V. Dakulagi, "Robust modified multiple signal classification algorithm for direction of arrival estimation," *Wireless Personal Communications*, vol. 115, no. 3, pp. 2535–2550, 2020.
[39] V. Dakulagi, "A new Nyström approximation based efficient coherent DOA estimator for radar applications," *AEU – International Journal of Electronics and Communications*, vol. 124, Art. no. 153328, 2020.
[40] M. Alagirisamy and M. Singh, "Efficient coherent direction-of-arrival estimation and realization using digital signal processor," *IEEE Transactions on Antennas and Propagation*, vol. 68, no. 9, pp. 6675–6682, Art. no. 9108563, 2020.
[41] M. Alagirisamy, "Adaptive beamformers for high-speed mobile communication," *Wireless Personal Communications*, vol. 113, no. 4, pp. 1691–1707, 2020.
[42] Md. Bakhar, "Advances in smart antenna systems for wireless communication," *Wireless Personal Communications*, vol. 110, no. 2, pp. 931–957, 2020.
[43] S. Wang, C. Gao, Q. Zhang, J. Cai, and B. Zong, "Research and experiment of radar signal support vector clustering sorting based on feature extraction and feature selection," *IEEE Access*, vol. 8, pp. 93322–93334, Art. no. 9090144, 2020.
[44] M. Alagirisamy, "Adaptive beamformers using 2D-novel ULA for cellular communication," *SN Applied Sciences*, vol. 1, no. 9, Art. no. 1001, 2019.
[45] Md. Bakhar, "Smart antenna system for DOA estimation using single snapshot," *Wireless Personal Communications*, vol. 107, no. 1, pp. 81–93, 2019.
[46] A. Noubade, A. Agasgere, P. Doddi, and K. Fatima, "Modified adaptive beamforming algorithms for 4G-LTE smart-phones," in *Advances in Intelligent Systems and Computing*, vol. 898, pp. 561–568, 2019.
[47] M. Bakhar, "Efficient blind beamforming algorithms for phased array and MIMO radar," *IETE Journal of Research*, vol. 64, no. 2, pp. 241–246, 2018.
[48] M. Bakhar, "A novel LMS beamformer for adaptive antenna array," *Procedia Computer Science*, vol. 115, pp. 94–100, 2017.
[49] M. Bakhar and R. M. Vani, "Robust blind beam formers for smart antenna system using window techniques," *Procedia Computer Science*, vol. 93, pp. 713–720, 2016.
[50] M. Bakhar, R. M. Vani, and P. V. Hunagund, "Implementation and optimization of modified MUSIC algorithm for high resolution DOA estimation," in *Proc. IEEE MTT-S Int. Microwave and RF Conf. (IMaRC)*, pp. 190–193, Art. no. 7038985, 2014.
[51] R. Raushan, S. Dutta, M. Theeb Alosaimi, and M. Villagómez-Galindo, "CUSE-TD Algorithm for Precision Detection of Coherent and Uncorrelated Signals," *IEEE Access*, vol. 13, pp. 11307–11319, 2025.



Vishal Ramola is an Associate Professor in the Department of Engineering and Technology at Uttarakhand Technical University, Dehradun, India. He has more than 27 years of academic and industry experience in Electronics and Communication Engineering, with research interests in VLSI design and low-power systems.



Manoj Kumar Panda is currently serving as Director, Women Institute of Technology, a constituent campus of Veer Madho Singh Bhandari Uttarakhand Technical University, Dehradun, India. He received his Ph.D. in Power and Control Systems from the Indian Institute of Technology Roorkee. He has over 21 years of teaching and two years of industry experience. He has published more than 50 research papers in reputed journals and conferences and holds five patents. His research interests include soft computing, renewable energy systems, control systems, and fuzzy control. He is a Senior Member of IEEE and a Fellow of the Institution of Engineers (India).